Molecular Biology of the Cell
Vol. 17, 1273–1285, March 2006

# Role of Numb in Dendritic Spine Development with a Cdc42 GEF Intersectin and EphB2[D]

**Takashi Nishimura,* Tomoya Yamaguchi,* Akinori Tokunaga,† Akitoshi Hara,* Tomonari Hamaguchi,* Katsuhiro Kato,* Akihiro Iwamatsu,‡ Hideyuki Okano,† and Kozo Kaibuchi***

*Department of Cell Pharmacology, Graduate School of Medicine, Nagoya University, Nagoya, Aichi 466-8550, Japan; †Department of Physiology, Keio University School of Medicine, Shinjuku-ku, Tokyo 160-8582, Japan; and ‡Central Laboratories for Key Technology, Kirin Brewery Company, Yokohama, Kanagawa 236-0004, Japan

Submitted August 1, 2005; Revised November 15, 2005; Accepted December 27, 2005
Monitoring Editor: Robert Parton

**Numb has been implicated in cortical neurogenesis during nervous system development, as a result of its asymmetric partitioning and antagonizing Notch signaling. Recent studies have revealed that Numb functions in clathrin-dependent endocytosis by binding to the AP-2 complex. Numb is also expressed in postmitotic neurons and plays a role in axonal growth. However, the functions of Numb in later stages of neuronal development remain unknown. Here, we report that Numb specifically localizes to dendritic spines in cultured hippocampal neurons and is implicated in dendritic spine morphogenesis, partially through the direct interaction with intersectin, a Cdc42 guanine nucleotide exchange factor (GEF). Intersectin functions as a multidomain adaptor for proteins involved in endocytosis and cytoskeletal regulation. Numb enhanced the GEF activity of intersectin toward Cdc42 in vivo. Expression of Numb or intersectin caused the elongation of spine neck, whereas knockdown of Numb and Numb-like decreased the protrusion density and its length. Furthermore, Numb formed a complex with EphB2 receptor-type tyrosine kinase and NMDA-type glutamate receptors. Knockdown of Numb suppressed the ephrin-B1-induced spine development and maturation. These results highlight a role of Numb for dendritic spine development and synaptic functions with intersectin and EphB2.**

## INTRODUCTION

The majority of excitatory synapses in the mammalian brain exist on specialized membrane protrusions known as dendritic spines (Harris, 1999; Hering and Sheng, 2001). Spines contain the machinery for neurotransmitter signaling and compartmentalize the biochemical and cell biological events that elicit synaptic modifications. During brain development, dendrites extend filopodia and those filopodia differentiate into mature spines capable of synaptic transmission through contact with complementary presynaptic sites (Yuste and Bonhoeffer, 2004). In the adult brain, filopodia and spines on dendrites continue to undergo morphological alternations that have been linked with learning and memory. Filopodia and spines are rich in F-actin and remodeling of the actin cytoskeleton controls the formation and motility of filopodia as well as the maturation of dendritic spines (Matus, 2000; Star *et al.*, 2002). Actin reorganization in dendritic spines is highly dynamic and responsive to synaptic signals, and actin remodeling is essential for the maintenance of long-term potentiation (Lamprecht and LeDoux, 2004). Several human mental retardation syndromes have been linked with altered morphology and number of dendritic spines (Fiala *et al.*, 2002). Recent studies suggest that the number and shape of dendritic spines are regulated by several proteins that either directly or indirectly modify the actin cytoskeleton, such as regulators of Rho family small GTPases and their downstream effectors (Luo, 2000; Govek *et al.*, 2005). However, the biochemical events that induce filopodia and remodel these structures into dendritic spines remain poorly understood.

The protein Numb was originally implicated in cell fate determination of peripheral and CNS development in *Drosophila* by antagonizing Notch signaling (Knoblich, 2001; Roegiers and Jan, 2004). Molecular studies of Numb homologues in vertebrates have identified two genes coding for Numb and Numb-like. Studies on double knockout mice revealed the importance of Numb and Numb-like in neural fate determination and differentiation by maintaining progenitor status or promoting neuronal fate (Petersen *et al.*, 2002; Li *et al.*, 2003). The structure of Numb protein suggests that it functions as an adapter protein to mediate the formation of multiprotein complexes. Numb has been implicated in clathrin-dependent endocytosis by binding to the AP-2 complex and Eps15 (Salcini *et al.*, 1997; Santolini *et al.*, 2000). In addition, Numb plays a role in neurite growth in postmitotic neurons (Sestan *et al.*, 1999; Shen *et al.*, 2002; Nishimura *et al.*, 2003). We previously reported that Numb accumulates at the tip of growing axons in cultured hippocampal neurons and serves a role in neurite growth by regulating endocytosis of L1, a neuronal cell adhesion mol-

This article was published online ahead of print in *MBC in Press* (http://www.molbiolcell.org/cgi/doi/10.1091/mbc.E05–07–0700) on January 4, 2006.

[D] The online version of this article contains supplemental material at *MBC Online* (http://www.molbiolcell.org).

Address correspondence to: Kozo Kaibuchi (kaibuchi@med.nagoya-u.ac.jp).

ecule, in the early stage of neuronal development (Nishimura *et al.*, 2003). However, localization and functions of Numb in the later stages of neuronal development remains unknown.

The results of our present study showed that Numb specifically localized to dendritic spines and controlled spine development in cultured hippocampal neurons. We identified a Cdc42-specific GEF intersectin as a Numb-binding protein by affinity column chromatography and found that Numb enhanced its GEF activity for filopodia formation. In addition, Numb formed a complex with EphB2 receptor and NMDA (*N*-methyl-D-aspartate)-type glutamate receptors at the postsynapse together with intersectin, which potentially links Numb to EphB and glutamate receptor signaling for synaptic development.

## MATERIALS AND METHODS

### *Materials and Chemicals*

The cDNA encoding human Numb was obtained as described previously (Nishimura *et al.*, 2003). The cDNA encoding full-length human intersectin-2 (KIAA1256) was a gift of Dr. T. Nagase (Kazusa DNA Research Institute, Chiba, Japan). Anti-Numb polyclonal antibody (PRR/3) was produced as described (Nishimura *et al.*, 2003). Monoclonal anti-intersectin-1 antibody, monoclonal anti-NR2B antibody, monoclonal anti-NR2 antibody, monoclonal anti-dynamin antibody, and monoclonal anti-RhoGDI antibody were from BD Biosciences PharMingen (San Diego, CA). Polyclonal anti-GFP antiserum, DiI, and Hoechst 33342 were from Molecular Probes (Eugene, OR). Monoclonal anti-GFP antibody and monoclonal anti-myc antibody were from Roche Diagnostics (Mannheim, Germany). Monoclonal anti-PSD95 antibody was from Affinity Bioreagents (Golden, CO). Polyclonal anti-GluR1 antibody was from Oncogene Research Products (San Diego, CA). Monoclonal anti-GST antibody, monoclonal anti-MAP-2 antibody, monoclonal anti-synaptophysin antibody, polyclonal anti-EphB2 antibody, polyclonal and monoclonal anti-human Fc antibody, and ephrin-B1-Fc were from Sigma (St. Louis, MO). Alexa 488, Alexa 568, and Alexa 647 conjugated secondary antibodies against mouse or rabbit IgG, and Fc fragment were from Jackson ImmunoResearch Laboratories (West Grove, PA). Other materials and chemicals were obtained from commercial sources.

### *Plasmid Constructs and Protein Purification*

Numb and intersectin fragments were amplified by PCR and subcloned into pGEX (Amersham Pharmacia Biotech, Buckinghamshire, United Kingdom), pRSET (Invitrogen, Carlsbad, CA), pCAGGS-myc, and pEGFP (BD Biosciences Clontech, San Jose, CA) vectors, respectively. All fragments were confirmed by DNA sequencing. Glutathione-*S*-transferase (GST)- and His-fusion proteins were produced in *Escherichia coli* BL21(DE3) cells and purified on glutathione-Sepharose 4B beads (Amersham) or nickel-resin (QIAGEN, Hilden, Germany), respectively.

### *Affinity Column Chromatography*

Total rat brain (P6 and P7) was homogenized in lysis buffer containing ionic detergents (10 mM Tris/HCl, 1 mM EDTA, 150 mM NaCl, 1.0% NP-40, 0.1% deocycholate, 0.1% SDS, 50 $\mu$g ml$^{-1}$ phenylmethylsulfonyl fluoride (PMSF), 10 $\mu$g ml$^{-1}$ leupeptin, pH 7.4) and then clarified by centrifugation at 100,000 $\times$ *g* for 30 min at 4°C. The soluble supernatants were loaded onto a glutathione-Sepharose affinity column on which GST, GST-Numb-PTB, or GST-Numb-PRR was immobilized. After washing the columns three times with lysis buffer, the bound proteins were subsequently eluted with lysis buffer containing 500 mM NaCl or 10 mM glutathione. The bound proteins were evaluated by SDS-PAGE followed by silver staining. To distinguish the specific binding proteins from *E. coli*-derived proteins, the eluates from the control columns without brain lysate were subjected to the same analysis and compared with the eluates from the column with extract.

### *Mass Spectrometry*

For mass spectrometry, the obtained eluates were dialyzed three times against distilled water and concentrated by freeze-drying. The concentrated samples were resolved by SDS-PAGE, followed by the transfer to PVDF membrane (Problot, Applied Biosystems, Foster City, CA). Each band was excised from the membrane, reduced, S-carboxymethylated, and digested in situ with *Achromabacter* protease I (a Lys-C). Molecular mass analysis of Lys-C fragments were performed by matrix-assisted laser desorption/ionization time-of-flight (MALDI-TOF) mass spectrometry using a PerSeptive Biosystem (Framingham, MA) Voyager-Delayed Extraction/RP. Proteins were identified by comparing the molecular weights determined by MALDI-TOF/mass spectrometry.

### *In Vitro Binding Assay*

GST-intersectin deletion mutants were separately immobilized onto glutathione-Sepharose 4B beads (Amersham). The immobilized beads were incubated with His-Numb deletion mutants in A-buffer (20 mM Tris/HCl, 1 mM EDTA, 1 mM dithiothreitol, 150 mM NaCl, 1% NP-40, pH 7.4) that contained 0.2 mg ml$^{-1}$ BSA, for 1 h at 4°C. The beads were washed five times with A-buffer, and the washed beads were suspended with SDS-PAGE sampling buffer. The bound proteins were subjected to an immunoblot analysis with anti-His antibody. For some experiments, GST-Numb or GST-intersectin protein immobilized beads were incubated with rat brain lysate as described above or with COS7 cell lysate transfected with the indicated plasmid, and the bound proteins were subjected to an immunoblot analysis with the indicated antibodies. GST-PAK-CRIB pulldown assay was performed as described previously (Nishimura *et al.*, 2005).

### *Subcellular Fractionation*

Synaptic plasma membranes were prepared essentially as described in Cho *et al.*, (1992). All procedures were performed at 4°C. All reagents included protease inhibitors (1 mM PMSF, 10 $\mu$g ml$^{-1}$ leupeptin) and protein phosphatase inhibitors (2 mM EGTA, 50 mM NaF, 1 mM sodium orthovanadate, 20 mM $\beta$-glycerophosphate). Adult rat cerebral cortices were homogenized in 10 volumes of HEPES-buffered sucrose (0.32 M sucrose, 4 mM HEPES/NaOH, pH 7.4) with a glass-Teflon homogenizer. The homogenate was centrifuged at 1000 $\times$ *g* for 10 min to remove the nuclear fraction and unbroken cells. The supernatant (S1) was then spun at 10,000 $\times$ *g* for 15 min to yield the crude synaptosomal fraction and the supernatant (S2). This pellet was resuspended in 10 vol of HEPES-buffered sucrose and then respun at 10,000 $\times$ *g* for another 15 min. The resulting pellet (P2) was lysed by hypoosmotic shock in water, rapidly adjusted to 4 mM HEPES, and mixed constantly for 30 min. The lysate was then centrifuged at 25,000 $\times$ *g* for 20 min to yield the supernatant (S3, crude synaptic vesicle fraction) and a pellet (P3, lysed synaptosomal membrane fraction). The pellet was resuspended in HEPES-buffered sucrose, carefully layered on top of a discontinuous gradient containing 0.8–1.0–1.2 M sucrose (top to bottom), and centrifuged at 150,000 $\times$ *g* for 2 h. The gradient yield a floating myelin fraction (G1), a light membrane fraction at the 0.8 M/1.0 M sucrose interface (G2), a synaptosomal plasma membrane (SPM) fraction at the 1.0 M/1.2 M sucrose interface (G3), and a mitochondrial fraction as the pellet (G4). Protein amounts of each fraction were measured by the BCA method (Pierce, Rockford, IL). Equal volumes of subcellular fractions and equal amounts of gradient fractions were subjected to Western blotting.

The postsynaptic density (PSD) fraction was isolated, prepared, and detergent-extracted, essentially as described (Blackstone *et al.*, 1992). The SPM were solubilized with 0.5% Triton X-100 in 50 mM HEPES/NaOH (pH 7.4) to yield the insoluble PSD Triton-1 pellet and supernatant. The PSD Triton-1 pellet was divided and extracted in a second round of 0.5% Triton X-100 or 3% *N*-lauroyl sarcosine to yield PSD Triton-2 and sarcosyl pellets and supernatants, respectively. Equal volumes of PSD pellets and supernatants were subjected to Western blotting.

### *Coimmunoprecipitation Experiment*

Rat brain (P6 and P7) was extracted by the addition of lysis buffer (20 mM Tris/HCl, 1 mM EDTA, 150 mM NaCl, 50 $\mu$g ml$^{-1}$ PMSF, 10 $\mu$g ml$^{-1}$ leupeptin, 1.0% NP-40, pH 7.4) and then clarified by centrifugation at 100,000 $\times$ *g* for 30 min at 4°C. The soluble supernatants were incubated with the indicated antibodies for 1 h at 4°C. The immunocomplexes were then precipitated with protein A-Sepharose 4B or protein G-Sepharose (Amersham). The immunocomplexes were washed three times with lysis buffer, eluted by boiling in sample buffer for SDS-PAGE, and then subjected to immunoblot analysis with the indicated antibodies. Alternatively, we used solubilized SPM lysate for coimmunoprecipitation, which was prepared by extracting the isolated SPM pellet as described above with lysis buffer containing ionic detergents.

### *Cell Culture and Immunofluorescence Analysis*

COS7 and N1E-115 cells were cultured in DMEM with 10% fetal bovine serum, and the transfection was performed using Lipofectamine (Invitrogen), according to the manufacturer's instructions. The culture of hippocampal neurons prepared from E18 rat embryos using papain was performed as described previously (Inagaki *et al.*, 2001). Dissociated neurons were plated on polylysine- and laminin-coated coverslips at a density of 5 $\times$ 10$^4$/well in 24-well plate and cultured in Neurobasal Medium (Invitrogen-Invitrogen) supplemented with B-27 (Invitrogen-Invitrogen) and 1 mM glutamine. Half of the culture medium was changed with fresh medium two times per week. Transfection of neurons was performed using a calcium phosphate method at the indicated period. Cells were fixed at the indicated period with 3.7% formaldehyde in phosphate-buffered saline (PBS) for 10 min at room temperature, followed by treatment for 10 min with 0.2% Triton X-100 that contained 2 mg ml$^{-1}$ BSA or cold methanol. The cells were observed with a confocal laser microscope system (LSM510; Carl Zeiss, Oberkochen, Germany) built around an Axiovert 100 M (Carl Zeiss) or an Axiophoto microscope (Carl Zeiss).

Activation of EphBs in cultured hippocampal neurons was performed as described previously (Henkemeyer *et al.*, 2003; Tolias *et al.*, 2005). To precluster before application to the neurons, ephrin-B1-Fc and control Fc were mixed with anti-human Fc antibody in a 1:2 ratio and incubated on ice for 1 h. Neurons were then stimulated with 500 ng/ml clustered ligands for 4 h at 37°C.

### *Immunohistochemistry*

Anesthetized adult rats were perfused intraaortically with 3.7% formaldehyde in PBS. Brains were removed and postfixed in the same fixative overnight at 4°C. 50 $\mu$m Vibratome sections were incubated with the indicated primary antibody overnight, then incubated with respective secondary antibody with DiI and Hoechst 33342 to visualize cell morphology and nucleus for 2 h, coverslipped with antifade mountant. Fluorescent images were acquired with a confocal laser microscope system (LSM510).

### *siRNA Transfection*

The oligonucleotide siRNA duplex was synthesized by Japan Bio Service (Saitama, Japan). We prepared several target sequences for Numb and Numb-like, and the sequences that showed the most efficient knockdown of Numb and Numb-like expression were used throughout the study. Sequences of siRNA were siNumb 5′-GGACCTCATAGTTGACCAG-3′, siNumb-like 5′-GGACCTGCTGGTAGACCAG-3′, and siScramble 5′-CAGTCGCGTTTGC-GACTGG-3′ as a control. The transfection of siRNA with the indicated plasmid in COS7 cells was carried out with Lipofectamine (Invitrogen). At 24 h after transfection, cells were harvested with SDS-PAGE sampling buffer. The transfection of siRNA with the indicated plasmid in primary neurons was carried out using the calcium phosphate method at the indicated period (Nishimura *et al.*, 2003). At 4 d after transfection, cells were fixed and analyzed.

### *Morphometric Measurements*

Measurement of dendritic protrusions was performed as described below. Neurons at the indicated period were fixed, and the transfected neurons were visualized by immunostaining of cotransfected GST with anti-GST polyclonal antibody. We used cotransfected GST protein as an unbiased cell-fill. Transfected neurons were chosen randomly for quantification from each coverslip in multiple assays and images were captured with LSM 510, using a 63× objective. Because dendritic protrusions often cross several *z* planes, we took 0.8–1 $\mu$m *z* series stacks from the bottom to the top of dendrites and used the LSM 510 software to generate image projections for quantitative analyses. The number of planes, typically 8–10, was chosen to cover the entire dendrite from top to bottom. Dendrites from cell body, 50 to 200 $\mu$m, were analyzed for quantification. All morphological experiments were repeated at least three times (n = 10–20 individual experiments). For quantification of protrusion density, protrusions to 6 $\mu$m in length were counted and expressed per 10 $\mu$m length of dendrite. Protrusion lengths were measured from the tip to the point where the protrusion met the dendritic shaft. Individual optical section images were used to verify each protrusion. Protrusions with a bulbous head wider than the base were scored as protrusions with a spine-head. For quantification of spine size and immunofluorescence intensity, images were analyzed using ImagePro analysis (Media Cybernetics, Silver Spring, MD) and Excel (Microsoft, Redmond, WA) by tracing cell body or dendritic spines according to the staining of cotransfected GST. The mean fluorescence intensity was determined by dividing the sum of all pixel intensities by the traced area after subtracting the background. All pooled images were analyzed using identical acquisition parameters. Student's *t* test was used to calculate the statistical significance.

## RESULTS

### *Numb Localization and Expression in Adult Brain*

To investigate the roles of Numb in mature neurons, we first examined the localization of Numb in the brain. Immunofluorescence staining of tissue sections revealed that Numb was widely expressed in the neurons in the adult rat brain and was enriched in the dendrites of neurons, as demonstrated by costaining with the dendrite marker MAP-2. DiI was used in order to trace the entire cell morphology in the sections. In the cerebral cortex, Numb staining concentrated at the MAP-2-positive dendrites of cortical neurons (Figure 1, A and D). In the CA1 region of hippocampus, Numb was found at high levels in the apical dendrites of pyramidal cells and at low levels in the cell body or interneurons (Figure 1, B and D). In the cerebellar cortex, Numb was expressed at high level in the dendrites of purkinje cells (Figure 1C). Expression of Numb in the neurons was further confirmed by costaining with the neuron marker NeuN (unpublished data). At high magnification, Numb were stained at puncta along with dendrites of layer V pyramidal neurons in the cerebral cortex and of the pyramidal neurons in the CA1 region of hippocampus (Figure 1D). These Numb puncta were largely overlapped with the postsynaptic marker PSD95, but not with the presynaptic marker synaptophysin. Immunoblot experiments showed that Numb protein was present in both embryonic and adult brain tissue, whereas PSD95 and synaptophysin proteins were up-regulated during development (Figure 1F). It remains unknown whether slight decrease of Numb in adult brain reflects the reduction of Numb protein levels per each cell or the reduction of Numb-positive cells per total cells in brain.

### *Numb Localizes at Dendritic Spines in Cultured Hippocampal Neurons*

To further investigate the subcellular localization of Numb in mature neurons, we examined the distribution of Numb in days in vitro (DIV) 21 cultured rat hippocampal neurons, which have mature synapses. Numb was immunostained at small or large puncta. Although small puncta were distributed throughout the cell body, axon, and dendrites, large puncta were specifically localized at the dendritic spines (Figure 1G). The presence of Numb at postsynaptic sites was confirmed by its colocalization with F-actin, which accumulates in spines, and its overlap localization with PSD-95, a major component of the PSD, but appeared not with synaptophysin (see Figure 4B). Further complementary biochemical studies confirmed that a proportion of endogenous Numb is localized at the postsynapse. We isolated SPM from rat cerebral cortices and subsequently prepared PSD fractions. Numb concentrated in SPM fractions with PSD-95 and NMDA-type glutamate receptor NR2B (see Figure 6A). Approximately 50% of Numb evidently existed in the insoluble PSD pellets even after two rounds of 0.5% Triton extraction. Further extraction of Triton-insoluble complexes with 3% *N*-lauroyl sarcosine solubilized ~30% of the Numb present, leaving 70% in the PSD core. As expected, PSD-95 is concentrated in all insoluble, detergent-extracted PSD pellets, whereas synaptophysin is totally solubilized upon treatment of SPM with Triton. Note, however, that the Numb antibody used here reacts with both Numb and Numb-like (unpublished data), so that we cannot discriminate the precise localization of each protein. Together, these results reveal a postsynaptic localization of Numb on dendritic spines.

### *Role of Numb for Dendritic Spine Development*

To examine the physiological roles of Numb on dendritic spines, we suppressed the expression of both Numb and Numb-like by siRNAs, because Numb and Numb-like have some redundant functions in mouse development and Numb-like is present in the developing nervous system, especially in postmitotic neurons (Zhong *et al.*, 1996; Petersen *et al.*, 2002; Li *et al.*, 2003). The efficacy of each siRNA in reducing Numb and Numb-like levels was first tested in COS7 cells, an easily transfectable cell line. Numb and Numb-like siRNAs were successful in reducing Numb and Numb-like levels, respectively (Figure 2A). We subsequently transfected Numb or Numb-like siRNA, or the mixture of Numb and Numb-like siRNAs with GST as a marker into dissociated DIV12 neurons and fixed them at DIV16. Immnocytochemical analysis of transfected neurons showed that the mixture of Numb and Numb-like siRNAs reduced the intensity of Numb immunolabeling relative to nearby

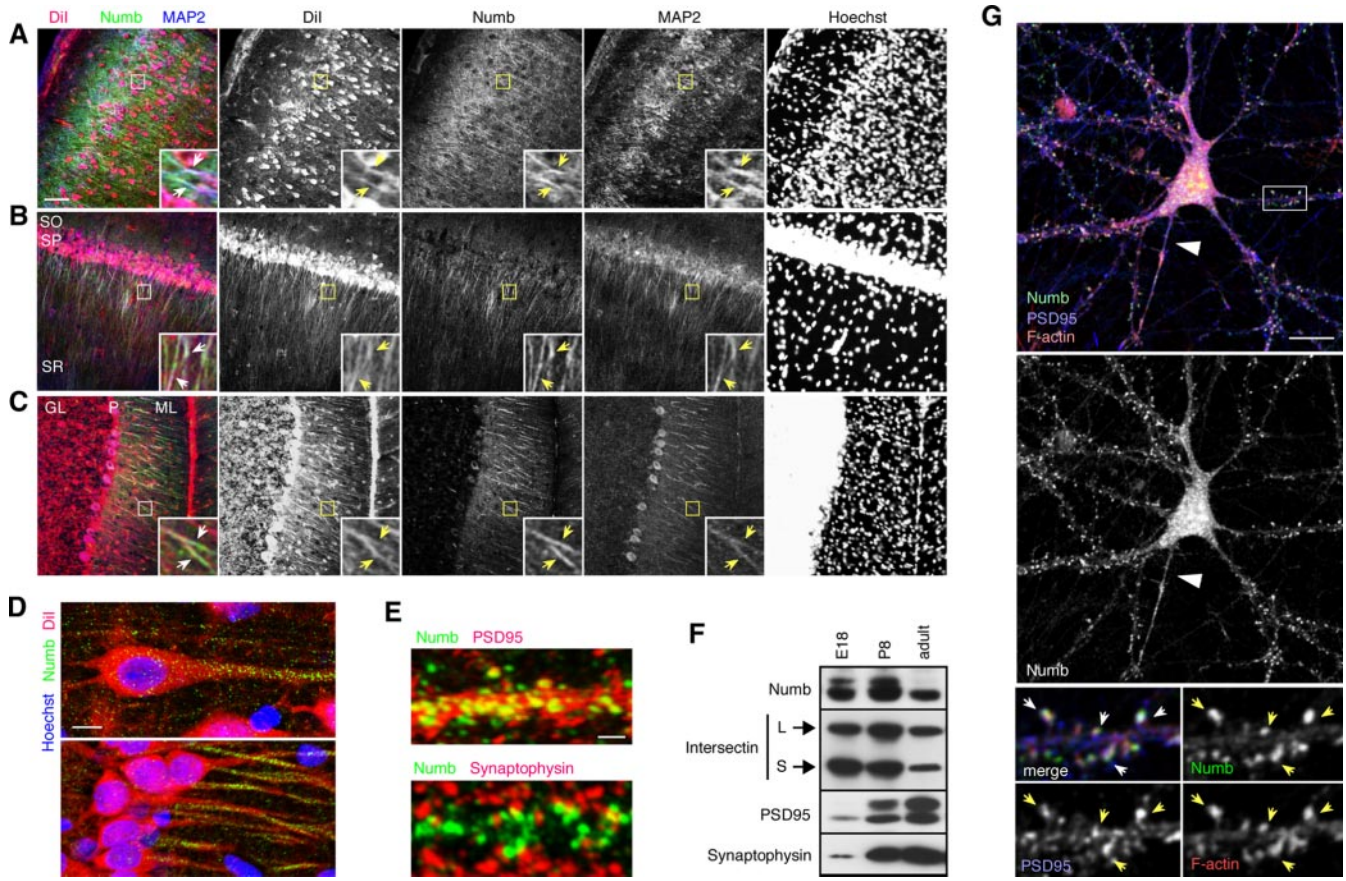


**Figure 1.** Localization of Numb in dendritic spines. (A–C) Localization of Numb in adult rat brain. Sections were incubated with anti-Numb antibody (green), anti-MAP-2 antibody (blue), DiI (red), and Hoechst. (A) cerebral cortex; (B) CA1 region of the hippocampus; and (C) cerebellar cortex. Insets, the enlarged images of the boxed area. Arrows, colocalization of Numb with MAP-2-positive dendrites. SO; stratum oriens, SP; stratum pyramidale, SR, stratum radiatum; GL, granular cell layer; P, Purkinje cells; ML, molecular layer. Bar, 50 $\mu$m. (D) High magnification images of the layer V pyramidal neurons of cerebral cortex (top panel) and the pyramidal neurons of the CA1 region (bottom panel). Red, green, and blue indicate DiI, Numb, and Hoechst, respectively. Bar, 10 $\mu$m. (E) Double-staining of Numb with PSD95 (top panel) and synaptophysin (bottom panel). High magnification images of the pyramidal neurons of the CA1 region are shown. Bar, 5 $\mu$m. (F) Expression of Numb in brain lysate. Equal amounts of the whole brain lysate at the indicated periods were subjected to the immunoblot analysis. (G) Localization of Numb in cultured rat hippocampal neurons. DIV21 mature neurons were fixed and then stained with anti-Numb antibody (green), anti-PSD95 antibody (blue), and phallodin (red) to stain F-actin. Enlarged images of the boxed area are shown (bottom). Arrowhead, the axon, as determined by its morphology; arrows, the dendritic spines where Numb colocalized with PSD95 and F-actin. Bar, 10 $\mu$m.

untransfected neurons, although the reduction was not complete (Figure 2B). Quantification analysis showed an ~10% reduction in the cell body transfected with Numb or Numb-like siRNA alone and a 60% reduction in the cells with the mixture of Numb and Numb-like siRNAs, compared with control cells (Figure 2C). However, the suppression of both Numb and Numb-like significantly reduced the number of filopodia-like protrusions on dendrite (Figure 2, D–F). Quantitative analysis showed that the suppression of Numb and Numb-like resulted in a decrease in the number of dendritic protrusions ($p < 0.005$, siScramble 4.25±0.24 per 10 $\mu$m of dendrites [mean ± SEM], n = 35, siNumb and siNumb-like 3.13 ± 0.19, n = 29) and in a decrease in the length of remaining protrusions ($p < 0.005$, siScramble 1.74 ± 0.02 $\mu$m, n = 860; siNumb and siNumb-like 1.53 ± 0.02 $\mu$m, n = 871; Figure 2, E and F). Furthermore, area of spine head was reduced in siNumb and siNumb-like transfected cells ($p < 0.005$, siScramble 0.80 ± 0.01 $\mu m^2$, n = 837, siNumb and siNumb-like 0.74 ± 0.01 $\mu m^2$, n = 911; Figure 2G). Percentage of the protrusions with mushroom-shaped head per total protrusions is 55.8 ± 3.2% of siScramble and 50.5 ± 2.8% of siNumb and siNumb-like ($p = 0.05$). Suppression of each protein alone did not affect the spine morphology under these conditions, suggesting that Numb and Numb-like have some redundant roles in spine development. To further examine the effect of Numb suppression on spine morphogenesis, we transfected Numb and Numb-like siRNAs into older DIV21 neurons that already had numerous mushroom-shaped spines and few filopodia and then analyzed the cells four days later. The density and length of dendritic spines in cells transfected with Numb and Numb-like siRNAs were indistinguishable from cells transfected with control siRNA or untransfected cells (Supplementary Information, Figure S1, A–C), suggesting that Numb and Numb-like are not required for maintaining the morphology of mature spines under these conditions. Taken together, these results indicate that reductions in Numb and Numb-like expression perturb spine development, suggesting that Numb proteins have a role in spine development.

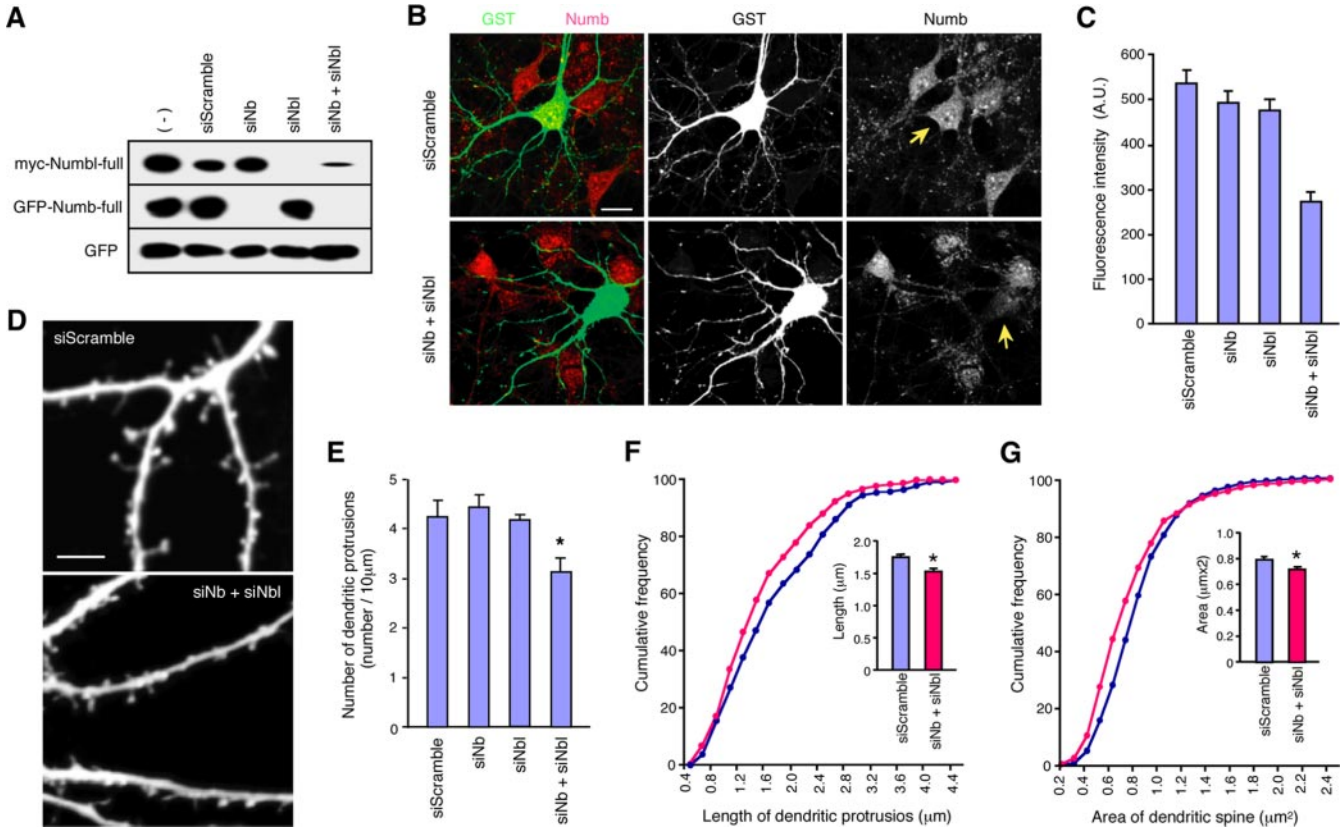


**Figure 2.** Suppression of Numb affects spine development. (A) Suppression of Numb and Numb-like by siRNAs in COS7 cells. COS7 cells were cotransfected with the indicated plasmid and siRNA. After 24 h of transfection, the expression level of each protein was analyzed by immunoblotting with anti-myc and anti-GEP antibody. (B) Suppression of Numb in hippocampal neurons. DIV12 primary neurons were transfected with the indicated siRNA along with the plasmid encoding GST as a fill. After 4 d of transfection, neurons were fixed and stained with anti-Numb antibody (red) and anti-GST antibody (green). Arrows indicate the transfected cells. Bar, 10 $\mu$m. (C) Quantitative analysis for the expression level of Numb. Fluorescence intensity of the cell body was measured to confirm the efficiency of Numb siRNAs. (D) Morphology of control and Numb-suppressed dendrites, as revealed by staining of cotransfected GST. Bar, 5 $\mu$m. (E) Number of dendritic protrusions in Numb-suppressed cells. Under the same conditions as those in D, the number of dendritic protrusions was counted. The data are means ± SE of pooled samples from at least three independent experiments. (F and G) The line graphs show the cumulative frequency distribution of protrusion lengths (F) and area of spine-head (G) for neurons transfected with siScramble (blue) or siNumb and siNumb-like (red). Insets show the mean spine length and mean area of spine-head for the two groups.

### *Identification of Intersectin as a Numb-binding Protein*

To investigate the molecular mechanisms for Numb on spine development, we next isolated Numb-binding proteins from postnatal brain by affinity column chromatography. Numb has a phosphotyrosine-binding (PTB) domain, proline-rich region (PRR), and tripeptide sequence motifs, such as Asn-Pro-Phe (NPF) and Asp-Pro-Phe (DPF) at the C-terminus (Figure 3C). We prepared detergent-extracted rat postnatal brain lysate, which contained ionic detergents to solubilize PSD proteins and loaded it onto a glutathione-Sepharose affinity column on which GST, GST-Numb-PTB, or GST-Numb-PRR was immobilized. The bound proteins were eluted by the addition of glutathione and were evaluated by SDS-PAGE followed by silver staining. Even in the presence of ionic detergents, major binding proteins with apparent molecular masses of ~105, 110, 115, 120, 165, 180, and 220 kDa were detected in the elution fraction from the GST-Numb-PRR affinity column but not from the GST or GST-Numb-PTB column (Figure 3A). To clarify the identity of these proteins, molecular mass analysis was performed. The molecular weights of peptides derived from p105, p110, p115, and p120 were found to be several isoforms of $\alpha$- or $\beta$-adaptin of the AP-2 complex, as reported (Santolini *et al.*, 2000); p180 was clathrin heavy chain; and p165 and p220 were intersectin-1 spicing variants, termed as short form (-S) and long form (-L), respectively.

Intersectin-S is ubiquitously expressed and consists of two Eps15 homology (EH) domains, a coiled-coil domain, and five Src homology 3 (SH3) domains (Figure 3E). Intersectin-L is predominantly expressed in the nervous system and includes three additional domains, a Dbl homology domain (DH), a pleckstrin homology domain (PH), and a C2 domain at the C-terminus. Intersectin binds several endocytic proteins, including dynamin, epsin, Eps15, and synaptojanin (O'Bryan *et al.*, 2001). The DH-PH domain of intersectin-L can function as a GEF for Cdc42 and can thereby modulate Cdc42/WASP-mediated regulation of the actin cytoskeleton (Hussain *et al.*, 2001). Intersectin-L has been reported to localize dendritic spines and mediate the EphB2 signaling on spine development, together with N-WASP and Cdc42 (Irie and Yamaguchi, 2002). The *Drosophila* homolog of intersectin, Dap160, plays a role in synaptic development and vesicle endocytosis (Koh *et al.*, 2004; Marie *et al.*, 2004).

These observations prompted us to examine whether Numb controls dendritic spine development through a Cdc42 GEF intersectin. We first examined whether Numb

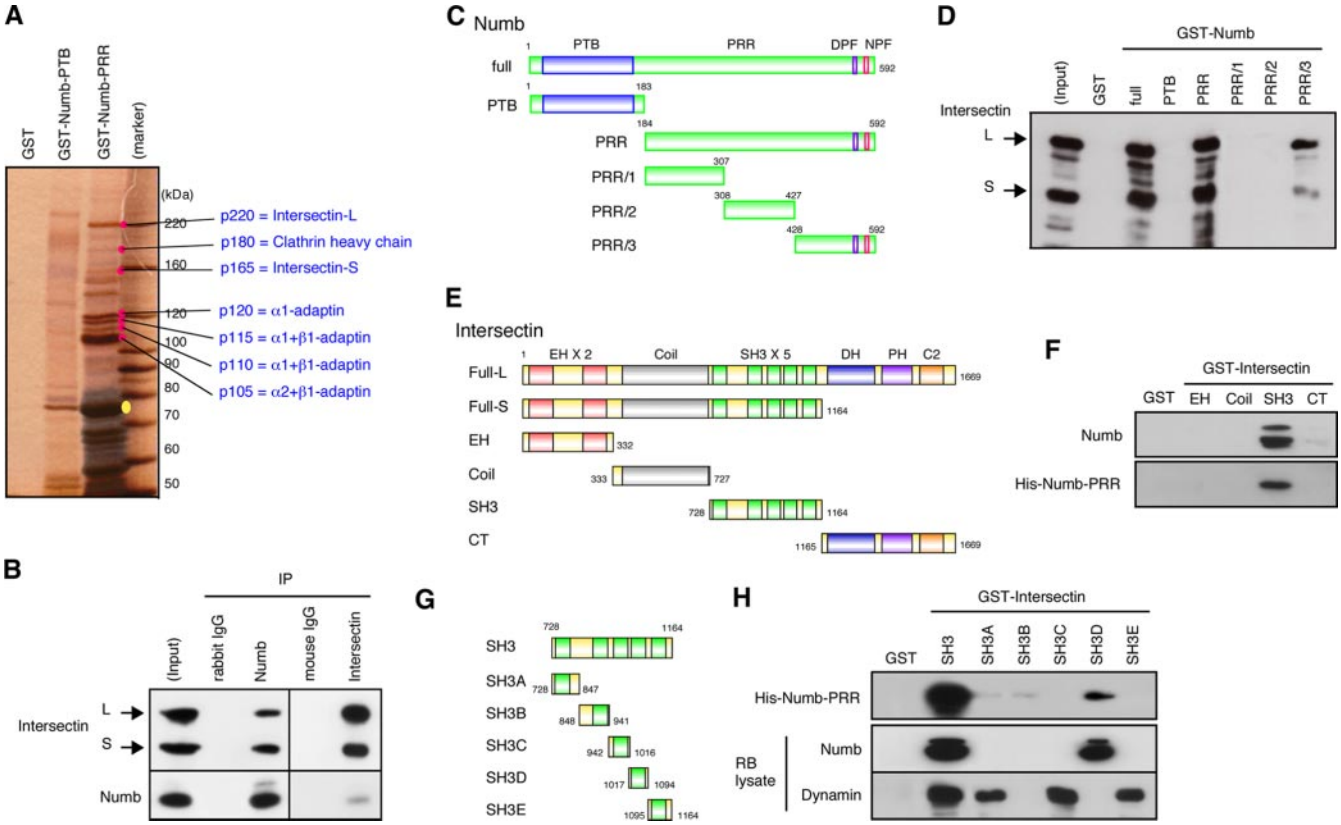


**Figure 3.** Interaction of Numb with intersectin in vivo and in vitro. (A) Isolation of Numb-binding proteins by affinity column chromatography. GST or GST-Numb fragment immobilized beads were incubated with rat brain lysate containing ionic detergents. The bound proteins were eluted by the addition of glutathione and analyzed by SDS-PAGE followed by silver staining. Red dots, the specific binding proteins to GST-Numb-PRR; yellow dot, the eluted GST-Numb-PRR protein. Identities of each bound protein, as revealed by molecular mass analysis, are shown on the right. (B) Coimmunoprecipitation of Numb and intersectin from rat brain lysate. Extract of developing rat brain was incubated with rabbit IgG, anti-Numb, mouse IgG, or anti-intersectin antibody. The immunoprecipitates were analyzed by immunoblotting with the indicated antibodies. (C) Domain structure and deletion constructs of Numb. Numbers refer to amino acid positions. (D) Identification of the binding region of Numb with intersectin. GST-Numb fragment immobilized beads were incubated with rat brain lysate. The bound proteins were analyzed by immunoblotting with anti-intersectin antibody. (E) Domain structure and deletion constructs of intersectin. Numbers refer to amino acid positions. (F) Mapping of the region in intersectin required for binding to Numb. GST-intersectin fragment immobilized beads were incubated with rat brain lysate or recombinant His-Numb-PRR. The bound proteins were analyzed by immunoblotting with anti-Numb antibody or anti-His antibody. (G) Deletion constructs of intersectin-SH3 domains. Numbers refer to amino acid positions. (H) Mapping of the region in intersectin-SH3 domains required for binding to Numb. GST-intersectin fragment immobilized beads were incubated with rat brain lysate or recombinant His-Numb-PRR. The bound proteins were analyzed by immunoblotting with anti-Numb antibody, anti-dynamin antibody, or anti-His antibody.

physiologically interacts with intersectin-1. When Numb was immunoprecipitated from rat brain lysate with anti-Numb antibody, the immunoreactive bands of intersectin-1-L and -S were detected in the immunoprecipitate (Figure 3B). Numb was reciprocally coimmunoprecipitated with anti-intersectin-1 specific antibody, although the recovery was low. Intersectin-1 has a closely related isoform, intersectin-2. We found that intersectin-2 also bound to Numb in vivo (unpublished data) and in vitro (see below), indicating that Numb interacts with both intersectin-1 and intersectin-2 isoforms. Hereafter, we use the term "intersectin" to indicate both "intersectin-1 and intersectin-2".

To examine the direct interaction and determine which region is responsible for the interaction with Numb and intersectin, an in vitro binding assay was performed. GST-Numb deletion-fragment immobilized beads were incubated with rat brain lysate to identify the intersectin binding region within Numb (Figure 3C). Endogenous intersectin-L and -S interacted with GST-Numb-full, GST-Numb-PRR, and GST-Numb-PRR/3, but not with GST-Numb-PRR/1 or PRR/2 (Figure 3D), although the recovery of intersectin to Numb-PRR/3 was significantly lower than those to GST-Numb-full and GST-Numb-PRR. These results suggest that the C-terminal region of Numb is responsible and required for the binding, but other regions appear to contribute to the high-affinity binding of intersectin to Numb.

We next produced four intersectin deletion fragments, termed intersectin-EH, coil, SH3, and CT (Figure 3E). Recombinant His-Numb-PRR directly interacted with GST-intersectin-SH3, but not with EH, coil, or CT (Figure 3F). Endogenous Numb specifically precipitated with GST-intersectin-SH3 from rat brain lysate. This result is consistent with those of affinity column chromatography: Numb precipitated both intersectin-L and intersectin-S, which contain SH3 domains. We then produced five deletion fragments that contain each SH3 domain (Figure 3G). His-Numb-PRR exclusively bound to GST-intersectin-SH3D (Figure 3H). Endogenous Numb also precipitated with GST-intersectin-SH3D. Under these conditions, dynamin, a known intersectin SH3 domain binding protein, interacted with GST-inter-

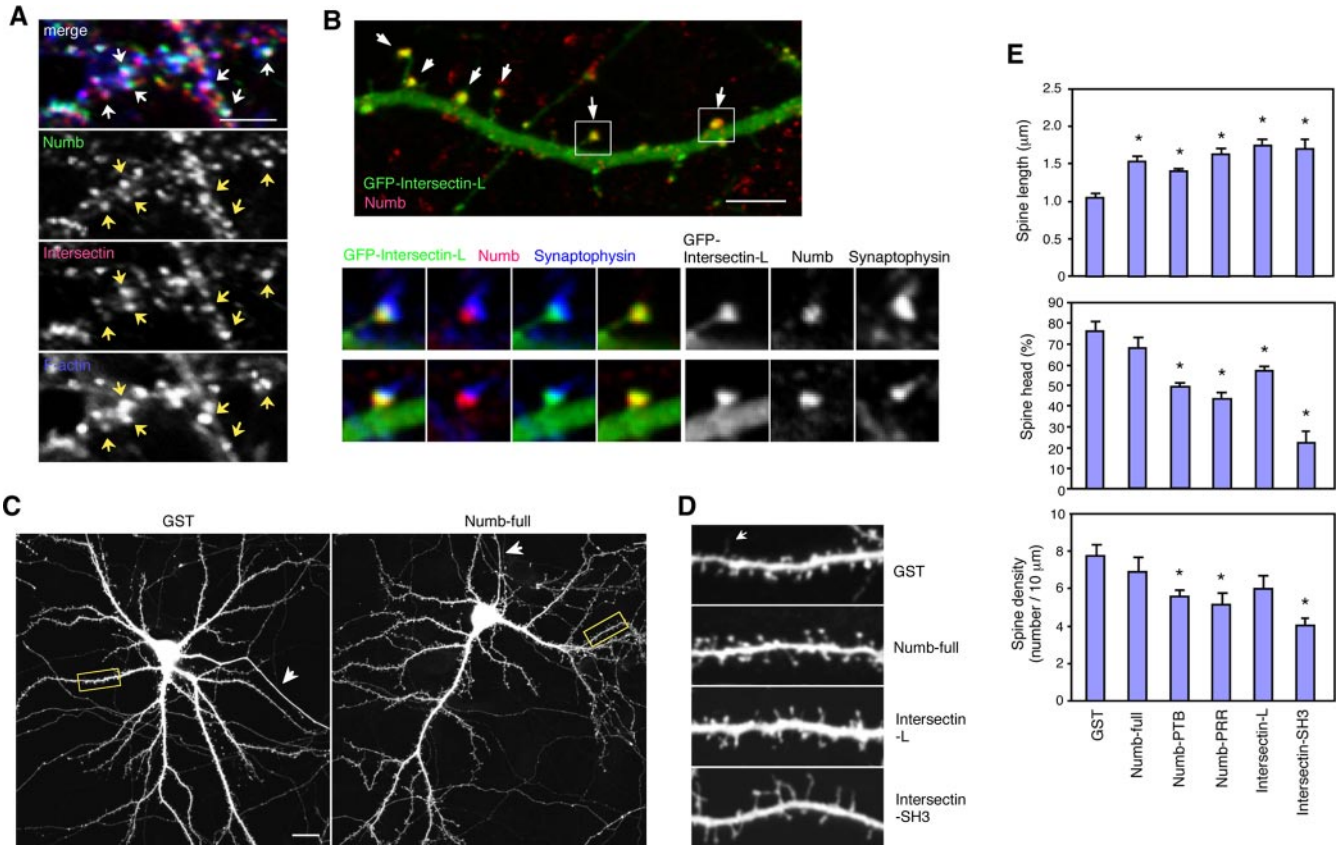


**Figure 4.** Effects of Numb and intersectin mutants on dendritic spine morphology in hippocampal neurons. (A) Colocalization of endogenous intersectin and Numb. DIV21 neurons were fixed and stained with anti-Numb antibody (green), anti-intersectin antibody (red), and phalloidin (blue). Arrows indicate dendritic spines where Numb and intersectin were colocalized. (B) Localization of Numb and intersectin at the postsynaptic site. DIV14 neurons were transfected with GFP-intersectin-L (green) and fixed at DIV21. Neurons were stained with anti-Numb antibody (red) and anti-synaptophysin antibody (blue). Arrows indicate the colocalization of Numb and GFP-intersectin-L at the dendritic spines. Enlarged images of single spine are shown below. Bars, 5 $\mu$m. (C) Cell morphology of control GST- and Numb-full-expressing neurons. DIV14 neurons were transfected with the indicated plasmid along with GST as a fill and fixed at DIV21. Enlarged images of the boxed area are shown in (D). Bar, 10 $\mu$m. (D) Morphology of dendritic spines. Under the same conditions those in (C), various constructs were examined. Arrow indicates a filopodial protrusion of control GST expressing neurons. (E) Quantitative analysis of the morphology of dendritic spines. Spine length, percentage of protrusions with a spine-head, and spine density were analyzed. The data are means ± SE of pooled samples from at least three independent experiments. Asterisks indicate a difference from the value of control GST-expressing cells at $p < 0.01$.

sectin-SH3A, -SH3C, and -SH3E, as reported previously (Yamabhai *et al.*, 1998; Zamanian and Kelly, 2003). Thus, the binding of Numb to intersectin-SH3D is specific and is different from that of known SH3 binding proteins, such as dynamin, SOS, and N-WASP (O'Bryan *et al.*, 2001). The C-terminal region of Numb contain several proline-rich regions, which serve as an SH3 domain binding motif, suggesting that intersectin could bind to these proline-rich regions of Numb.

### *Numb and Intersectin Affect Spine Morphogenesis*

We next examined the subcellular localization of Numb and intersectin. Numb and intersectin bind to several proteins implicated in clathrin-dependent endocytosis and localize to clathrin-coated structures (CCSs; Santolini *et al.*, 2000; O'Bryan *et al.*, 2001). Endogenous Numb colocalized with intersectin-S at CCSs in Hela cells (Supplementary Information, Figure S1D), which express only intersectin-S (unpublished data). In DIV21 cultured hippocampal neurons, which express both intersectin-L and -S, intersectin colocalized with Numb and F-actin at dendritic spines (Figure 4A). The ectopically expressed GFP-intersectin-L localized to the dendritic spines and was colocalized with Numb. Consistent with a postsynaptic localization, GFP-intersectin-L and endogenous Numb in dendritic spines closely juxtaposed immunolabeling with the presynaptic marker synaptophysin (Figure 4B). Similar to the subcellular distribution of Numb, both intersectin-L and -S concentrated in the SPM fraction (data shown below in Figure 6A). Approximately 50% of intersectin-L remained in the Triton-insoluble PSD pellets, whereas almost all intersectin-S was Triton soluble, suggesting a postsynaptic localization of intersectin-L on dendritic spines and intersectin-L playing a role in synaptic development.

We next assessed the effects of Numb and intersectin mutants on dendritic spine morphogenesis. We transiently transfected in DIV14 cultured hippocampal neurons and observed the morphology of spines at DIV21. We found that control GST-transfected DIV21 neurons have acquired their characteristic dendritic branching pattern and displayed numerous protrusions from their dendrites. Although a minority of these protrusions were filopodial (long and headless),

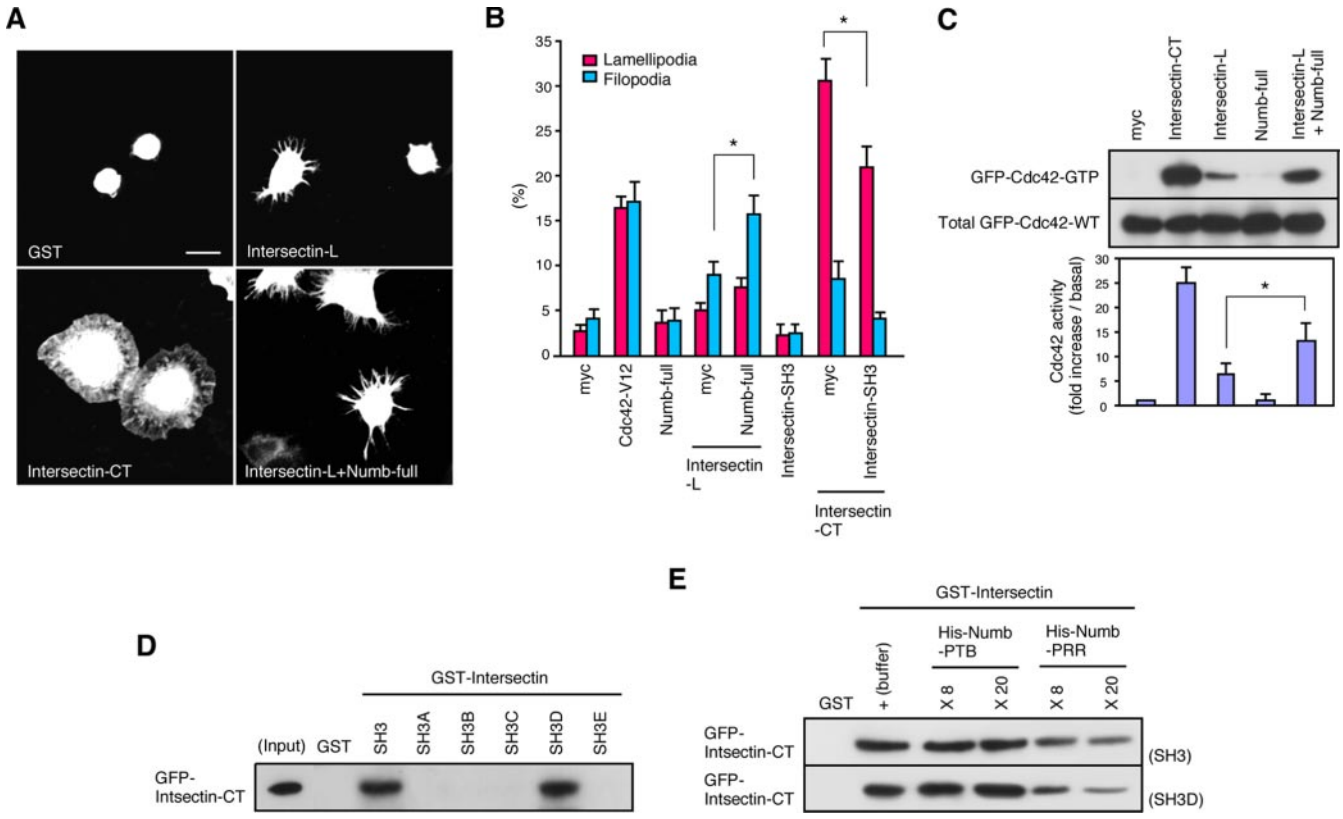


**Figure 5.** Numb enhances intersectin GEF activity toward Cdc42 in vivo. (A) Filopodia and lamellipodia formation by intersectin mutants in N1E-115 cells. Cells were transfected with the indicated constructs, fixed 24 h after transfection, and stained with anti-GST antibody to visualize the transfected cells by immunostaining of cotransfected GST. Bar, 20 $\mu$m. (B) Effects of Numb and intersectin mutants on cell morphology. Under the same conditions as those in A, GST-positive cells were scored for the presence of filopodia or lamellipodia. The data are means $\pm$ SD of at least three independent experiments. Asterisks indicate a statistical difference at $p < 0.01$. (C) Activation of Cdc42 by Numb and intersectin. COS7 cells transfected with the indicated constructs and GFP-Cdc42-WT were incubated with GST-PAK-CRIB to precipitate the GTP form of Cdc42. The amounts of GTP-bound and total Cdc42 were determined by immunoblotting with anti-GFP antibody (top). The ratio of GTP-Cdc42 to total Cdc42 is shown on the bottom. (D) Intramolecular interaction between intersectin-SH3 and intersectin-CT. GST-intersectin immobilized beads were incubated with COS7 cell lysate expressing GFP-intersectin-CT. Bound proteins were analyzed by immunoblotting with anti-GFP antibody. (E) Competition assay of Numb with intramolecular interaction of intersectin. GST, GST-intersectin-SH3, and GST-intersectin-SH3D immobilized beads were incubated with a mixture of COS7 cell lysate expressing GFP-intersectin-CT and excess recombinant His-Numb-PTB or His-Numb-PRR. Bound proteins were analyzed by immunoblotting with anti-GFP antibody. Number indicates the amount of His-Numb proteins against GST-intersectin proteins.

a large fraction had a well-defined neck and head structure, characteristic of mature spines (Figure 4, C and D). We measured the length and number of dendritic protrusions. Expression of Numb-full increased the spine length but slightly reduced the number of spines (Figure 4, C–E). The majority of the Numb-full-induced spines had a normal spine-head, suggesting that Numb-full increases the spine-neck but does not affect the spine-head morphology. Expression of intersectin-L showed similar effects to Numb-full. In contrast, expression of intersectin-SH3 and Numb-PRR, which bind to each other, increased the spine length and reduced the spine density, suggesting that these mutants impair spine development. Because intersectin-SH3 and Numb-PRR bind to several partners, we could not conclude that the effects are dependent on the perturbation of the binding between Numb and intersectin. Expression of Numb-PTB caused the similar defects, suggesting that N-terminal region of Numb is also implicated in spine development. Taking into account the effects of Numb suppression on spine number and spine length, these results raise the possibility that Numb regulates spine morphogenesis together with intersectin at dendritic spines.

### *Numb Enhances the GEF Activity of Intersectin In Vivo*

Given the importance of actin dynamics in dendritic spine morphogenesis and synaptic transmission, we examined whether Numb binding to intersectin affects the GEF activity of intersectin toward Cdc42. To test this possibility, we first examined the effect of Numb and intersectin-L on cell morphology in N1E-115 neuroblastoma, which express only intersectin-S (unpublished data). Expression of constitutively active Cdc42 induces filopodia as well as Rac-dependent lamellipodia through the PAR complex and STEF/Tiam1 Rac GEFs (Nishimura *et al.*, 2005). Intersectin-CT, which contains isolated DH-PH domains, more efficiently induced lamellipodia and slightly induced filopodia under these conditions (Figure 5, A and B). Of note, intersectin-CT had Cdc42-specific GEF activity in vitro (unpublished data; Hussain *et al.*, 2001; Zamanian and Kelly, 2003), suggesting that Cdc42 activation by intersectin-CT is converted to Rac activation for lamellipodia. Expression of full-length intersectin-L slightly induced filopodia, whereas control GST or Numb-full did not. However, intersectin-L more efficiently induced filopodia in the presence of overexpressed Numb-

full. To confirm the activation levels of Cdc42 in vivo, we performed a GST-PAK-CRIB pulldown assay, which specifically precipitates Cdc42-GTP. We found that intersectin-CT strongly induced Cdc42-GTP levels, whereas full-length intersectin-L only slightly induced it (Figure 5C). The expression of Numb-full had no effect on Cdc42-GTP levels. Coexpression of Numb-full with intersectin-L increased the Cdc42-GTP levels relative to intersectin-L alone. These results indicate that Numb enhances intersectin GEF activity toward Cdc42 in vivo and that GEF activity of intersectin is regulated by other regions. It has been reported that the GEF activity of the DH-PH domain of intersectin-L is negatively regulated by its adjacent SH3 domains intramolecularly (Zamanian and Kelly, 2003). Consistent with this observation, intersectin-CT-induced lamellipodia were partially inhibited by the coexpression of intersectin-SH3 in N1E-115 cells (Figure 5B). Isolated GFP-intersectin-CT expressed in COS7 cells bound to intersectin-SH3 and the isolated SH3D domain selectively (Figure 5D). Thus, Numb could compete with the intramolecular interaction between SH3D and DH-PH domains of intersectin, thereby enhancing its GEF activity. To test this hypothesis, a competition assay was performed. Excess His-Numb-PRR, but not His-Numb-PTB, competed with the interaction between GST-intersectin-SH3 or GST-intersectin-SH3D and GFP-intersectin-CT in a dose-dependent manner (Figure 5E). Taken together, these results suggest that Numb controls intersectin GEF activity toward Cdc42 by inducing the conformational change of intersectin.

### *Numb Interacts with EphB2 and NMDA-Type Glutamate Receptors at Dendritic Spines*

Because synaptic development and remodeling is closely associated with the signaling of neurotransmitter receptors, we considered whether Numb might associate with neurotransmitter and signaling receptors at the postsynapse. Intersectin plays a role in synaptic development under ephrin-B-EphB signaling (Irie and Yamaguchi, 2002). Analysis of EphBs mutant mice has demonstrated that ephrinB-EphBs signaling is important not only in normal dendritic spine development but also in plasticity and behaviors (Grunwald *et al.*, 2001; Henderson *et al.*, 2001; Henkemeyer *et al.*, 2003). EphB receptors have been reported to regulate synaptic plasticity through extracellular interaction with NMDA receptors (Dalva *et al.*, 2000; Henderson *et al.*, 2001; Takasu *et al.*, 2002). Thus, we incubated GST-Numb and GST-intersectin fragment immobilized beads with rat brain lysate to examine the interaction of NMDA-receptors and EphB2 with Numb and intersectin. Both NMDA-type glutamate receptors NR1 and NR2B were efficiently precipitated with GST-Numb-full, GST-Numb-PTB, GST-Numb-PRR, and GST-intersectin-SH3 even in the presence of ionic detergents (Figure 6B). However, the AMPA-type glutamate receptor GluR1 was not precipitated. EphB2 was precipitated with GST-Numb-PTB and weakly precipitated with GST-Numb-full and GST-intersectin-SH3 under these conditions. NMDA receptors directly interact with PSD95 to maintain the signaling of glutamate in PSD (McGee and Bredt, 2003). Interestingly, GST-Numb fragments did not precipitate PSD95 in the presence of NMDA receptors, whereas GST-intersectin-SH3 did. To examine the physiological association of Numb with these receptors, we prepared isolated SPM lysate, which was solubilized with ionic-detergent, and precipitated Numb-interacting receptors by anti-Numb antibody. Numb immunoprecipitated NR1, NR2B, and EphB2 from the solubilized SPM fraction (Figure 6C). Again, Numb did not immunoprecipitate PSD95 in the presence of NMDA-Rs. Low recoveries of each transmembrane receptor might be due to the dissociation of the protein-protein interaction by ionic detergent. However, EphB2 was Triton soluble and was not present in the PSD core (Figure 6A), suggesting that biochemical properties of EphB2 and NMDA receptors at the postsynapse seem to be different.

### *Numb Is Required for Ephrin-B1-induced Spine Development*

Ephrin-B activation of EphB receptors induces the coclustering of EphB receptors and NMDA receptors in the postsynaptic membrane (Henkemeyer *et al.*, 2003; Tolias *et al.*, 2005). To examine whether Numb colocalizes with the EphB2 in these clusters in response to EphB activation, we treated DIV10 neurons with aggregated ephrin-B1-Fc. We found that ephrin-B1 stimulation promoted the clustering of Numb with EphB2 along dendrites (Figure 6D), suggesting that Numb is recruited to EphB2 receptor complexes after EphB activation. Taken together, these observations indicate that Numb physiologically associates with EphB2 receptors and may be implicated in the signaling for spine development.

We next analyzed whether the suppression of Numb affects the localization of Numb-binding partners at spines in normal growth conditions. We measured the average fluorescence intensity of intersectin, EphB2, NR1, and PSD95 per spine area in DIV14, because the suppression of Numb decreased the area of spine-head (Figure 2G). The localization of intersectin at spines was not affected by the suppression of Numb (Figure 7, A and B), suggesting that Numb is not required for the targeting of intersectin to spines. On the other hand, fluorescence intensity of EphB2, NR1, and PSD95 was reduced in Numb-suppressed cells, whereas the defects were not remarkable. These results suggest that Numb is partially implicated in the localization of EphB2, NR1, and PSD95 at spines, although our results cannot distinguish between the localization of receptors at spine surface and that at intracellular vesicles. Finally, we examined the functional significance of Numb in the EphB signaling for dendritic spine development and synaptic maturation. We treated clustered ephrin-B1 with DIV12 neurons previously transfected with GST to visualize their morphology. Treatment with clustered ephrin-B activates Cdc42 and thereby results in an increase in the number and size of dendritic protrusions (Irie and Yamaguchi, 2002; Henkemeyer *et al.*, 2003; Penzes *et al.*, 2003). Some were long and thin protrusions, resembling filopodia, some were short and wide protrusions, and others had necks and mushroom-shaped heads, resembling mature spines (Figure 7C). Quantitative analysis indicated that ephrin-B1 increased the number of dendritic protrusions and PSD95-containing spines with mushroom-shaped heads (Figure 7, D and E). Suppression of Numb proteins by siRNAs partially impaired the ephrin-B1-induced protrusion formation. Suppression of Numb reduced the percentage of the protrusions with mushroom-shaped head (siScramble, 67 $\pm$ 3.5%; siNumb and siNumb-like, 57 $\pm$ 4.1%, $p < 0.05$) and also reduced the percentage of PSD95-positive spines per total spines (Figure 7E). Taken together, these results suggest that Numb controls synaptic development and maturation both upstream and downstream of ephrin-B1, presumably with intersectin and Cdc42.

## DISCUSSION

Our studies, for the first time, highlight a role of Numb in the development of dendritic spines in mammalian postmitotic neurons. Numb puncta were enriched at dendrites of neurons in brain tissue, although we do not know whether

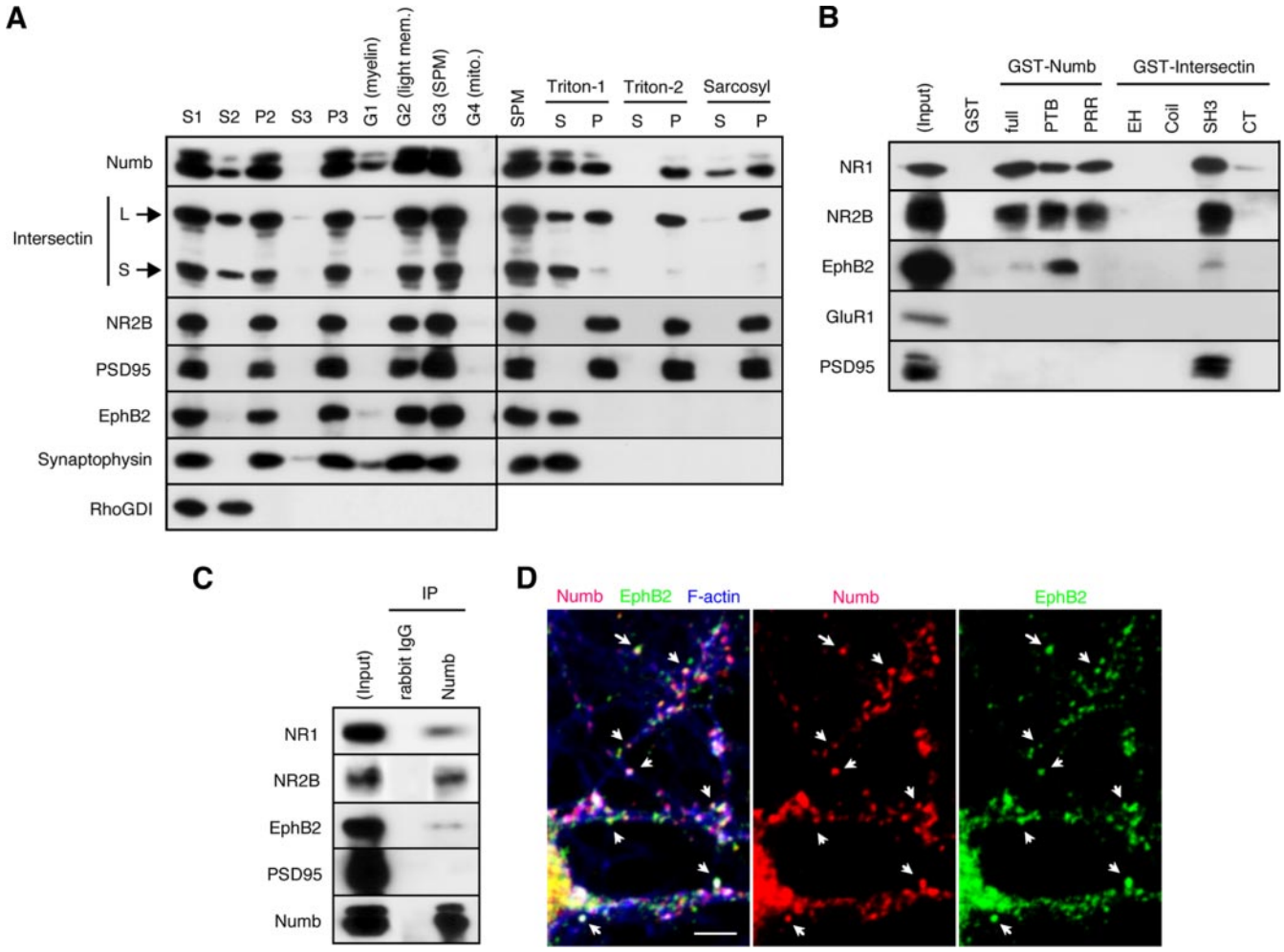


**Figure 6.** Numb associates with EphB2 and NMDA receptors at dendritic spines. (A) Isolation of PSD fraction from rat adult cerebral cortices. Subcellular fractionation was performed to isolate the SPM fraction. Aliquots of subcellular fractions (see *Materials and Methods*) were analyzed by immunoblotting with the indicated antibodies. RhoGDI was used as a control for supernatant. G1 to G4 fractions of the density gradient contain floating myelin (myelin), light membrane mixture (light mem.), synaptosomal plasma membrane (SPM), and mitochondrial pellet (mito.) from top to bottom. SPM were further extracted in 0.5% Triton X-100 to yield the PSD Triton-1 pellet (P) and supernatant (S). The PSD Triton-1-P was extracted in 0.5% Triton X-100 again or 3% *N*-lauroyl sarcosine to yield PSD Triton-2 and sarcosyl pellets and supernatants, respectively. (B) Interaction of Numb and intersectin with EphB2 and NMDA receptors. GST-Numb or GST-intersectin fragment immobilized beads were incubated with rat brain lysate. Bound proteins were analyzed by immunoblotting with the indicated antibodies. (C) Coimmunoprecipitation of Numb with EphB2 and NMDA receptors. Solubilized SPM lysate was incubated with rabbit IgG or anti-Numb antibody. Immunoprecipitates were analyzed by immunoblotting with the indicated antibodies. (D) Colocalization of Numb with clustered EphB2 receptor. DIV14 neurons were treated with clustered ephrin-B1-Fc for 4 h and then fixed. Neurons were stained with anti-Numb antibody (red), anti-EphB2 antibody (green), and phalloidin (blue). Arrows indicate the colocalization of Numb with EphB2 at dendritic spines. Bar, 5 $\mu$m.

these Numb puncta mean clustering at dendritic spines or intracellular vesicles. Immunostaining in dissociated hippocampal neurons indicates that Numb accumulates at dendritic spines. It remains to be clarified whether accumulation of Numb at dendritic surface precedes spine formation or not. It will be interesting to examine whether electrical and neurotransmitter stimulation affect Numb expression and localization in spines. Double-staining with pre- and postsynaptic markers indicates that Numb evidently localizes to postsynapse. However, we cannot ignore that Numb localizes to presynaptic terminals and functions in recycling of synaptic vesicles at this stage. Further ultrastructural analysis will be required to understand the precise localization of Numb in mature neurons, such as presynaptic terminal, postsynaptic membrane, shaft, and endocytic structures.

We isolated a Cdc42 GEF intersectin as a Numb-binding protein at the postsynapse, and that Numb modulated its GEF activity toward Cdc42 for filopodia formation. Numb competed with the intramolecular interaction of intersectin, and therefore Numb binding to intersectin seems to activate its GEF activity toward Cdc42. Intersectin binds to Eps15 (Sengar *et al.*, 1999), which in turn binds to Numb through a different region. Intersectin also binds to dynamin (Okamoto *et al.*, 1999; Sengar *et al.*, 1999), which could form a complex with clathrin and the AP-2 complex. We also identified clathrin-heavy chain together with the AP-2 complex in the elution fraction of GST-Numb-PRR. However, Numb point

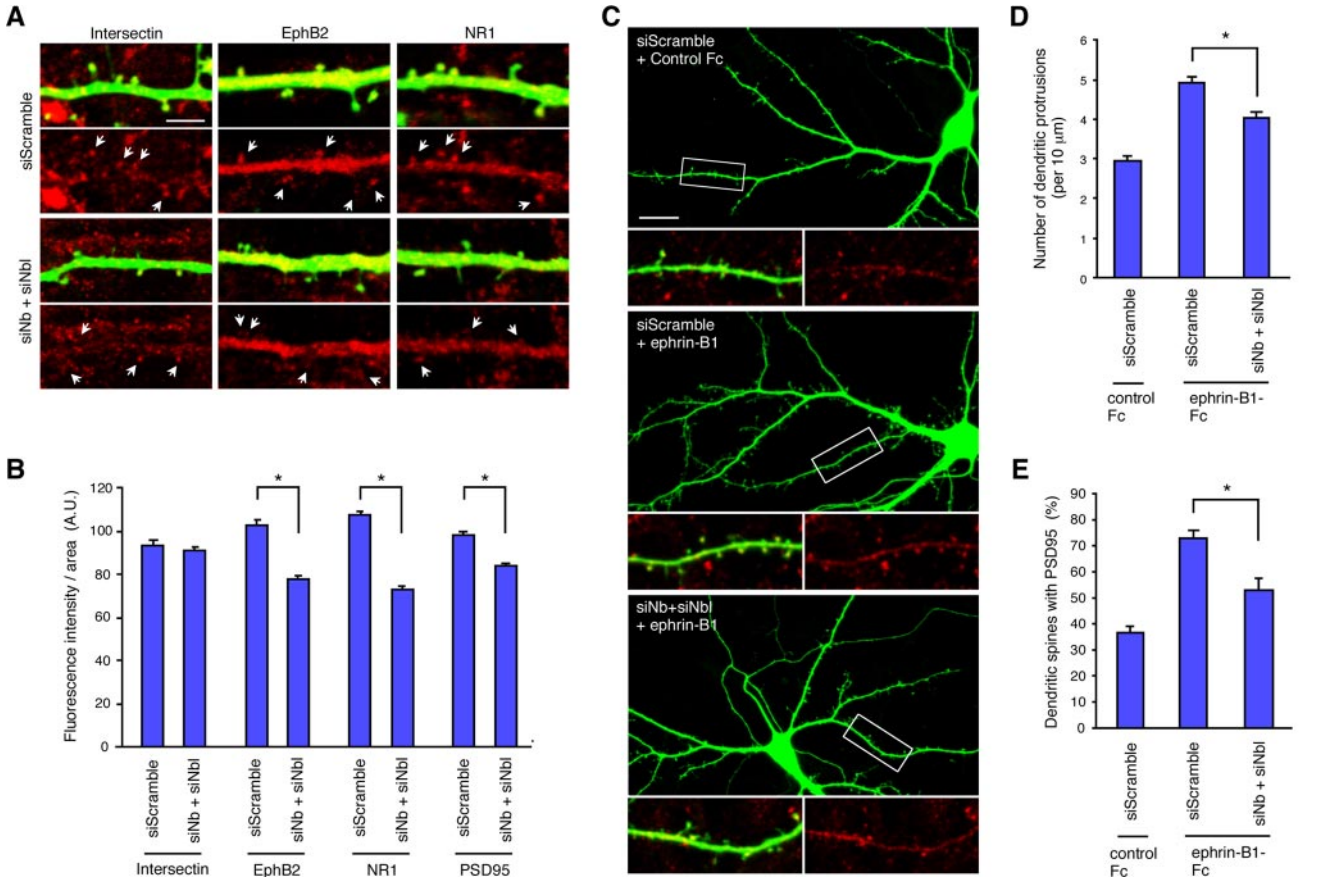


**Figure 7.** Suppression of Numb impairs ephrin-B1-induced spine development and maturation. (A) The effects of Numb suppression on the localization of intersectin, EphB2, and NR1 on dendritic spines. DIV10 neurons were transfected with indicated siRNA along with GST. Four days after transfection, neurons were fixed and stained with anti-GST (green) and the indicated antibodies (red). Arrows indicate the position of dendritic spines. Bar, 5 $\mu$m. (B) Quantification of average fluorescence intensity in spines. Average fluorescence intensity of each protein per spine area was analyzed in neurons transfected with siScramble and neurons transfected with siNumb and siNumb-like. The data are means $\pm$ SE of pooled samples. Asterisks indicate a difference from the value of siScramble-transfected neurons at $p < 0.001$. (C) Changes in dendritic protrusions after stimulation of clustered ephrin-B1-Fc. DIV10 neurons were transfected with indicated siRNA along with GST. Four days after transfection, neurons were treated with clustered ephrin-B1-Fc or control Fc for 4 h and then fixed. Neurons were stained with anti-GST antibody (green) and anti-PSD95 antibody (red). Enlarged images of the boxed area are shown below. Bar, 10 $\mu$m. (D), (E) Quantitative analysis of the morphology of dendritic protrusions. Number of dendritic protrusions (D) and PSD95-positive protrusions with a spine-head (E) were analyzed. The data are means $\pm$ SE of pooled samples from at least three independent experiments. Asterisks indicate a difference from the value of siScramble-transfected neurons with ephrin-B1-Fc at $p < 0.01$.

mutants (Numb-DLA/NLA) unable to bind to AP-2 and Eps15 abolished the binding to clathrin (unpublished data), suggesting that Numb indirectly interacts with clathrin, presumably through the AP-2 complex. Thus, Numb and intersectin could form a multimolecular complex with several endocytic proteins without direct interaction. Intersectin has a C2 domain next to the DH-PH domain, although calcium does not appear to affect its GEF activity at least in vitro (Zamanian and Kelly, 2003). Numb can be phosphorylated by calcium/calmodulin-dependent protein kinases (CaMKs; Tokumitsu *et al.*, 2005). Thus, calcium influx in spines may affect its GEF activity or the Numb-intersectin binding, causing alternations in spine structure. Taken together, these observations raise the possibility that Numb-intersectin binding for Cdc42 activation is regulated by receptor signaling and/or sequential bindings of endocytic proteins at the postsynapse.

The suppression of Numb reduced the protrusion density, protrusion length, and spine-head area, although the defects are not remarkable. The relatively minor defects on spine morphology could be due to the inefficient knockdown of Numb by siRNAs in our assay conditions. We found that Numb associated with EphB2 and NMDA receptors, thus possibly mediating the signaling of EphB2 and NMDA receptors for dendritic spine formation and maturation. This possibility is supported by the findings that Numb is recruited to the EphB2 receptor complex upon stimulation of clustered ephrin-B1-Fc. Ephrin-B stimulation induces Cdc42 activation, presumably through intersectin and N-WASP (Irie and Yamaguchi, 2002). The suppression of Numb impaired the ephrin-B1-induced spine morphogenesis. However, the defects could be partially due to the mislocalization of EphB2 receptor, because the suppression of Numb reduced the intensity of EphB2 at spines. Numb may function in the stabilization of EphB2 and NMDA-receptors at spines or in the recruitment of these receptors to spines directly or indirectly. Thus, it could be possible that Numb is implicated in both the initial localization of receptors in spines and the downstream signaling of their ligands to modulate spine morphogenesis and reinforce synaptic activity.

Rho family small GTPases play a critical role in the development and maintenance of spine morphology in mature neurons (Nakayama *et al.*, 2000; Govek *et al.*, 2005). In our mass-spectral and immunoblot analyses in the sample of immunoprecipitate of anti-Numb antibody, Rac GEF Tiam1 and dual Rho GEF kalirin were coimmunoprecipitated with anti-Numb antibody, in addition to the Cdc42 GEF intersectin (unpublished data). Kalirin mediates the ephrin-B-EphB signaling for the induction of dendritic spine morphogenesis by activating Rac and its effector PAK (Penzes *et al.*, 2003). Tiam1 plays a role in ephrin-B1 induced neurite growth (Tanaka *et al.*, 2004). Furthermore, Tiam1 has been reported to interact with NMDA receptors and mediate the NMDA receptor-dependent dendritic development (Tolias *et al.*, 2005). Thus, Numb appears to function in several signaling pathways at the postsynapse downstream of glutamate and ephrin-B signaling. It should be noted that targeted deletion of Numb and Numb-like in sensory neurons exhibited severe neurological deficits (Huang *et al.*, 2005). In addition to the defects in axon arborization, Numb may be implicated in spine development and synaptic activity in the neurological deficits. Further work will be required to dissect the roles of Numb, which couples sequential activation of Rho GTPases to endocytosis of neurotransmitter receptors for spine development and subsequent synaptic activity.

## ACKNOWLEDGMENTS

We thank members of Kaibuchi and Okano lab, K. Fujii, and N. Nishimura for technical help and T. Ishii for secretarial assistance. This research was supported in part by Grants-in-Aid for Scientific Research, a Grant-in-Aid for Creative Scientific Research, and The 21st Century Center of Excellence Program from the Ministry of Education, Culture, Sports, Science and Technology of Japan; a Research Grant for Nervous and Mental Disorders from the Ministry of Health, Labor and Welfare; and a grant from The Pharmaceuticals and Medical Devices Agency. T. N. is a Research Fellow of the Japan Society for the Promotion of Science.

## REFERENCES

Blackstone, C. D., Moss, S. J., Martin, L. J., Levey, A. I., Price, D. L., and Huganir, R. L. (1992). Biochemical characterization and localization of a non-*N*-methyl-D-aspartate glutamate receptor in rat brain. J. Neurochem. *58*, 1118–1126.

Cho, K. O., Hunt, C. A., and Kennedy, M. B. (1992). The rat brain postsynaptic density fraction contains a homolog of the *Drosophila* discs-large tumor suppressor protein. Neuron *9*, 929–942.

Dalva, M. B., Takasu, M. A., Lin, M. Z., Shamah, S. M., Hu, L., Gale, N. W., and Greenberg, M. E. (2000). EphB receptors interact with NMDA receptors and regulate excitatory synapse formation. Cell *103*, 945–956.

Fiala, J. C., Spacek, J., and Harris, K. M. (2002). Dendritic spine pathology: cause or consequence of neurological disorders? Brain Res. Brain Res. Rev. *39*, 29–54.

Govek, E. E., Newey, S. E., and Van Aelst, L. (2005). The role of the Rho GTPases in neuronal development. Genes Dev. *19*, 1–49.

Grunwald, I. C., Korte, M., Wolfer, D., Wilkinson, G. A., Unsicker, K., Lipp, H. P., Bonhoeffer, T., and Klein, R. (2001). Kinase-independent requirement of EphB2 receptors in hippocampal synaptic plasticity. Neuron *32*, 1027–1040.

Harris, K. M. (1999). Structure, development, and plasticity of dendritic spines. Curr. Opin. Neurobiol. *9*, 343–348.

Henderson, J. T., Georgiou, J., Jia, Z., Robertson, J., Elowe, S., Roder, J. C., and Pawson, T. (2001). The receptor tyrosine kinase EphB2 regulates NMDA-dependent synaptic function. Neuron *32*, 1041–1056.

Henkemeyer, M., Itkis, O. S., Ngo, M., Hickmott, P. W., and Ethell, I. M. (2003). Multiple EphB receptor tyrosine kinases shape dendritic spines in the hippocampus. J. Cell Biol. *163*, 1313–1326.

Hering, H., and Sheng, M. (2001). Dendritic spines: structure, dynamics and regulation. Nat. Rev. Neurosci. *2*, 880–888.

Huang, E. J., Li, H., Tang, A. A., Wiggins, A. K., Neve, R. L., Zhong, W., Jan, L. Y., and Jan, Y. N. (2005). Targeted deletion of *numb* and *numblike* in sensory neurons reveals their essential functions in axon arborization. Genes Dev. *19*, 138–151.

Hussain, N. K. *et al.* (2001). Endocytic protein intersectin-l regulates actin assembly via Cdc42 and N-WASP. Nat. Cell Biol. *3*, 927–932.

Inagaki, N., Chihara, K., Arimura, N., Kawano, Y., Matsuo, N., Nishimura, T., Amano, M., and Kaibuchi, K. (2001). CRMP-2 induces axons in cultured hippocampal neurons. Nat. Neurosci. *4*, 781–782.

Irie, F., and Yamaguchi, Y. (2002). EphB receptors regulate dendritic spine development via intersectin, Cdc42 and N-WASP. Nat. Neurosci. *5*, 1117–1118.

Knoblich, J. A. (2001). Asymmetric cell division during animal development. Nat. Rev. Mol. Cell. Biol. *2*, 11–20.

Koh, T. W., Verstreken, P., and Bellen, H. J. (2004). Dap160/intersectin acts as a stabilizing scaffold required for synaptic development and vesicle endocytosis. Neuron *43*, 193–205.

Lamprecht, R., and LeDoux, J. (2004). Structural plasticity and memory. Nat. Rev. Neurosci. *5*, 45–54.

Li, H. S., Wang, D., Sheng, Q., Schonemann, M. D., Gorski, J. A., Jones, K. R., Temple, S., Jan, L. Y., and Jan, Y. N. (2003). Inactivation of Numb and Numblike in embryonic dorsal forebrain impairs neurogenesis and disrupts cortical morphogenesis. Neuron *40*, 1105–1118.

Luo, L. (2000). Rho GTPases in neuronal morphogenesis. Nat. Rev. Neurosci. *1*, 173–180.

Marie, B., Sweeney, S. T., Poskanzer, K. E., Roos, J., Kelly, R. B., and Davis, G. W. (2004). Dap160/intersectin scaffolds the periactive zone to achieve high-fidelity endocytosis and normal synaptic growth. Neuron *43*, 207–219.

Matus, A. (2000). Actin-based plasticity in dendritic spines. Science *290*, 754–758.

McGee, A. W., and Bredt, D. S. (2003). Assembly and plasticity of the glutamatergic postsynaptic specialization. Curr. Opin. Neurobiol. *13*, 111–118.

Nakayama, A. Y., Harms, M. B., and Luo, L. (2000). Small GTPases Rac and Rho in the maintenance of dendritic spines and branches in hippocampal pyramidal neurons. J. Neurosci. *20*, 5329–5338.

Nishimura, T., Fukata, Y., Kato, K., Yamaguchi, T., Matsuura, Y., Kamiguchi, H., and Kaibuchi, K. (2003). CRMP-2 regulates polarized Numb-mediated endocytosis for axon growth. Nat. Cell Biol. *5*, 819–826.

Nishimura, T., Yamaguchi, T., Kato, K., Yoshizawa, M., Nabeshima, Y., Ohno, S., Hoshino, M., and Kaibuchi, K. (2005). PAR-6-PAR-3 mediates Cdc42-induced Rac activation through the Rac GEFs STEF/Tiam1. Nat. Cell Biol. *7*, 270–277.

O'Bryan, J. P., Mohney, R. P., and Oldham, C. E. (2001). Mitogenesis and endocytosis: what's at the intersection? Oncogene *20*, 6300–6308.

Okamoto, M., Schoch, S., and Sudhof, T. C. (1999). EHSH1/intersectin, a protein that contains EH and SH3 domains and binds to dynamin and SNAP-25. A protein connection between exocytosis and endocytosis? J. Biol. Chem. *274*, 18446–18454.

Penzes, P., Beeser, A., Chernoff, J., Schiller, M. R., Eipper, B. A., Mains, R. E., and Huganir, R. L. (2003). Rapid induction of dendritic spine morphogenesis by trans-synaptic ephrinB-EphB receptor activation of the Rho-GEF kalirin. Neuron *37*, 263–274.

Petersen, P. H., Zou, K., Hwang, J. K., Jan, Y. N., and Zhong, W. (2002). Progenitor cell maintenance requires numb and numblike during mouse neurogenesis. Nature *419*, 929–934.

Roegiers, F., and Jan, Y. N. (2004). Asymmetric cell division. Curr. Opin. Cell Biol. *16*, 195–205.

Salcini, A. E., Confalonieri, S., Doria, M., Santolini, E., Tassi, E., Minenkova, O., Cesareni, G., Pelicci, P. G., and Di Fiore, P. P. (1997). Binding specificity and in vivo targets of the EH domain, a novel protein-protein interaction module. Genes Dev. *11*, 2239–2249.

Santolini, E., Puri, C., Salcini, A. E., Gagliani, M. C., Pelicci, P. G., Tacchetti, C., and Di Fiore, P. P. (2000). Numb is an endocytic protein. J. Cell Biol. *151*, 1345–1352.

Sengar, A. S., Wang, W., Bishay, J., Cohen, S., and Egan, S. E. (1999). The EH and SH3 domain Ese proteins regulate endocytosis by linking to dynamin and Eps15. EMBO J. *18*, 1159–1171.

Sestan, N., Artavanis-Tsakonas, S., and Rakic, P. (1999). Contact-dependent inhibition of cortical neurite growth mediated by Notch signaling. Science *286*, 741–746.

Shen, Q., Zhong, W., Jan, Y. N., and Temple, S. (2002). Asymmetric Numb distribution is critical for asymmetric cell division of mouse cerebral cortical stem cells and neuroblasts. Development *129*, 4843–4853.

Star, E. N., Kwiatkowski, D. J., and Murthy, V. N. (2002). Rapid turnover of actin in dendritic spines and its regulation by activity. Nat. Neurosci. *5*, 239–246.

Tanaka, M., Ohashi, R., Nakamura, R., Shinmura, K., Kamo, T., Sakai, R., and Sugimura, H. (2004). Tiam1 mediates neurite outgrowth induced by ephrin-B1 and EphA2. EMBO J. *23*, 1075–1088.

Takasu, M. A., Dalva, M. B., Zigmond, R. E., and Greenberg, M. E. (2002). Modulation of NMDA receptor-dependent calcium influx and gene expression through EphB receptors. Science *295*, 491–495.

Tokumitsu, H., Hatano, N., Inuzuka, H., Sueyoshi, Y., Yokokura, S., Ichimura, T., Nozaki, N., and Kobayashi, R. (2005). Phosphorylation of Numb family proteins. Possible involvement of Ca2+/calmodulin-dependent protein kinases. J. Biol. Chem. *280*, 35108–35118.

Tolias, K. F., Bikoff, J. B., Burette, A., Paradis, S., Harrar, D., Tavazoie, S., Weinberg, R. J., and Greenberg, M. E. (2005). The Rac1-GEF Tiam1 couples the NMDA receptor to the activity-dependent development of dendritic arbors and spines. Neuron *45*, 525–538.

Yamabhai, M., Hoffman, N. G., Hardison, N. L., McPherson, P. S., Castagnoli, L., Cesareni, G., and Kay, B. K. (1998). Intersectin, a novel adaptor protein with two Eps15 homology and five Src homology 3 domains. J. Biol. Chem. *273*, 31401–31407.

Yuste, R., and Bonhoeffer, T. (2004). Genesis of dendritic spines: insights from ultrastructural and imaging studies. Nat. Rev. Neurosci. *5*, 24–34.

Zamanian, J. L., and Kelly, R. B. (2003). Intersectin 1L guanine nucleotide exchange activity is regulated by adjacent src homology 3 domains that are also involved in endocytosis. Mol. Biol. Cell *14*, 1624–1637.

Zhong, W., Jiang, M. M., Weinmaster, G., Jan, L. Y., and Jan, Y. N. (1996). Differential expression of mammalian Numb, Numblike and Notch1 suggests distinct roles during mouse cortical neurogenesis. Development *124*, 1887–1897.